Thermochimica Acta, 118 (1987) 35–55
Elsevier Science Publishers B.V., Amsterdam – Printed in The Netherlands

PHASES AND THERMAL DECOMPOSITION CHARACTERISTICS OF HYDRO-SODALITES $Na_{6+x}[AlSiO_4]_6(OH)_x \cdot nH_2O$

J. FELSCHE and S. LUGER

Fakultät für Chemie, Universität Konstanz, Postfach 5560, D-7750 Konstanz (F.R.G.)

(Received 23 January 1987)

ABSTRACT

Reinvestigation of the hydro-sodalite system does not verify the solid solution character of the series in respect to a steady variation in properties of the samples. Thermoanalyses of carefully prepared pure phases reveal an antagonistic volume/concentration effect of hydrate water in the two end-member series $Na_8[AlSiO_4]_6(OH)_2 \cdot nH_2O$, $0 \leqslant n \leqslant 4$ ("basic series") and $Na_6[AlSiO_4]_6 \cdot nH_2O$, $0 < n \leqslant 8$ ("non-basic series"), however. Thermogravimetry and X-ray diffraction heating experiments confirm partial collapse of the sodalite framework upon dehydration of phases of the basic hydro-sodalites which is the common behaviour of framework compounds in decomposition or ion exchange experiments. In contrast, phases of the non-basic sodalite hydrate series $Na_6[AlSiO_4]_6 \cdot nH_2O$ show significant expansion of the alumino-silicate framework, when H_2O ($0 < n \leqslant 8$) is released at temperatures of 350 – 450 K under open system conditions. This antagonistic effect on the sodalite type host lattice is discussed in terms of hydrogen bonding, which has been verified by supplementary neutron diffraction analyses for the non-basic hydro-sodalites, distinctively.

From IR and X-ray diffraction heating experiments strong evidence is given for the dynamic nature of interactions between all the non-framework constituents with increasing activation barriers for the hydrogen, oxygen and sodium atoms, respectively. The truncated octahedral geometry of the sodalite cage in the given 1 : 1 alumino-silicate matrix controls the corresponding interactions, which result in some new stereochemical features of the aqueous hydroxyl groupings $[O_nH_{2n-1}]^-$ in the basic hydro-sodalite phases with different hydrate water contents. Samples of partially leached samples with intermediate concentrations of NaOH, $0 < x < 2$, show decomposition into mixed phase samples of the basic ($x = 2$) and of the non-basic ($x = 0$) type of hydro-sodalite, respectively. The data on the given β-cage chemistry are discussed in terms of some corresponding findings with zeolites A and Y.

INTRODUCTION

We reinvestigate the family of hydro-sodalite phases with special interest in the interactions of the non-framework and framework constituents, which might be controlled by hydrogen bonding. The results may contribute to a more thorough understanding of reactions in the field of intra-zeolite chemistry with special attention to the β-cage constitution of the structurally related zeolites A, X/Y.

Our experiments are based on the preliminary results of former investigations, which showed fundamental influence on the developments of characterization and synthesis of porous tecto-silicates [1–4]. In this study we apply a large variety of suitable methods of up-to-date solid state analysis with special attention to pure phase samples. The experiments are focussed on the full scope of chemical composition of the hydro-sodalite phases $Na_{6+x}[AlSiO_4]_6(OH)_x \cdot nH_2O$ with corresponding ranges of $0 \leqslant x \leqslant 2$ and $0 \leqslant n \leqslant 8$ being aware of the problems of non-single crystal analysis given by the non-artificiality of our methods of preparation of mild hydrothermal conditions. At first we accept the poly-crystalline nature of our synthetic products for the benefit of the larger range in the chemical composition of our hydro-sodalite samples.

The more recent analytical studies on hydro-sodalites are predominantly concerned with phases of rather narrow composition $Na_8[AlSiO_4]_6(OH)_2 \cdot nH_2O$ with $1.7 < n < 2.2$ [5–8]. Because of the model character of the $[4^6 6^8]$ sodalite cage chemistry for some more complicated zeolite or clathralite systems we want to contribute to the analytical knowledge on the interactions of the non-framework constituents of hydrogen, oxygen and sodium atoms on the mechanistic level [9].

In this paper we report on the synthesis of the different phases of the hydro-sodalite family and on the thermoanalytical data of the two end-member series $Na_8[AlSiO_4]_6(OH)_2 \cdot nH_2O$ and $Na_6[AlSiO_4]_6 \cdot nH_2O$ in particular. Complementary analytical data on individual phases from X-ray/neutron scattering or NMR- and ESR-spectroscopic experiments are published elsewhere.

EXPERIMENTAL

Samples of hydroxo-sodalite hydrates $Na_8[AlSiO_4]_6(OH)_2 \cdot nH_2O$, $3 < n \leqslant 4$, have been prepared from mixtures of kaolinite (Fluka 60609) and 12–16 M solutions of NaOH (Merck 43565) at temperatures 350–420 K in 10 cm^3 teflon-coated steel autoclaves. Pure phase character of individual batches has been controlled by X-ray Guinier powder diffraction photographs. Batches showing foreign phases such as nepheline hydrate or cancrinite have been excluded from subsequent ion exchange experiments or thermoanalytical procedures.

Sodalite hydrates $Na_6[AlSiO_4]_6 \cdot nH_2O$, $6 < n \leqslant 8$, have been obtained from autoclave exchange experiments at 135 °C employing compositions $Na_8[AlSiO_4]_6 \cdot nH_2O$, $3 < n \leqslant 4$, as starting materials and corresponding H_2O concentrations. In order to specify for hydrate water in subsequent thermoanalytical runs, weakly absorbed surface water has been retained by maturing samples under standardized desiccator conditions. Separation from amorphous materials, which do not show up in Guinier diffraction control

experiments, appears to be one of the most serious problems in the preparation of pure hydro-sodalite samples. Certain features of TG- or DTG-curves in subsequent thermoanalytical runs allowed for exclusion of misleading data, however.

Any manipulation of samples during synthesis, analytical procedures or for transfer to further equipment had to be carried out under air-exclusion conditions. Standardized polycrystalline samples of grain size 0.1–1.0 μm have been prepared for the subsequent thermoanalytical experiments. Commercially available zeolite A of composition $Na_{12}(AlO_2)_{12}(SiO_2)_{12} \cdot 27H_2O$ (EGA-Chemie, 20-859-0) has been provided for comparing the thermoanalytical properties of related zeolites.

X-ray diffraction data have been obtained with a Guinier powder diffraction system (600 Huber, Rimsting, Cu K_{α_1} radiation, $2\theta = 5–85°$, relative intensities I/I_0 through peak integration of 0.001° step scans, LSQS-refinement of lattice constants). Diffraction heating photographs at temperatures 298–1100 K have been taken on a high-resolution Guinier camera system advanced from the Enraf-Nonius type Simon-heating device (heating rate 10 K h^{-1}, N_2-atmosphere, 99.999%, SiO_2 silica capillaries ϕ 0.3 mm, gold standard $a_0 = 4.0786(5)$ at 299 K (Gray 1972)). Thermoanalytical experiments have been carried out on a Netzsch-thermoanalyzer STA-429 employing DTA, thermogravimetry and simultaneous mass spectrometry (Pt-cruci-

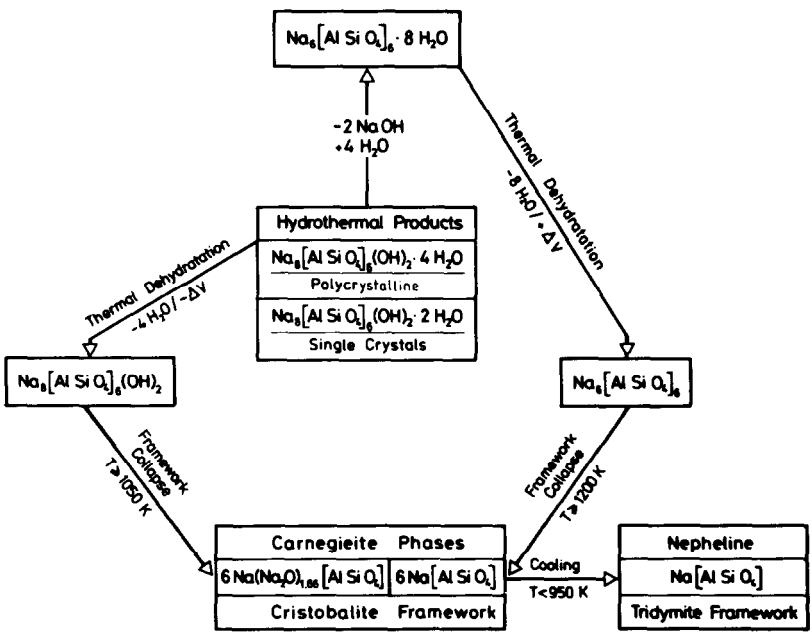

Fig. 1. Particular hydro-sodalite phases and experimental procedures of the different approaches of the reinvestigation of the hydro-sodalite family.

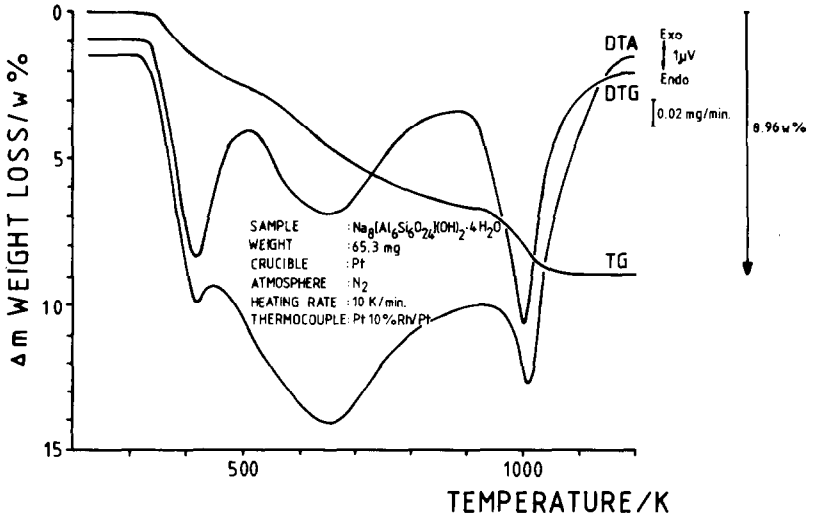

Fig. 2. Simultaneous thermoanalysis, TG(DTG)–DTA of the top-hydrate phase of the basic hydro-sodalite series, $Na_8[AlSiO_4]_6(OH)_2 \cdot 4H_2O$.

bles, heating rate 0.2–10 K min^{-1}, N_2-atmosphere, 99.999%, Balzers QMG-511). The special leak system for normal pressure runs has been described previously [10].

IR-transmission experiments at elevated temperatures have been carried out in a special device [11] attached to a regular double beam spectrometer

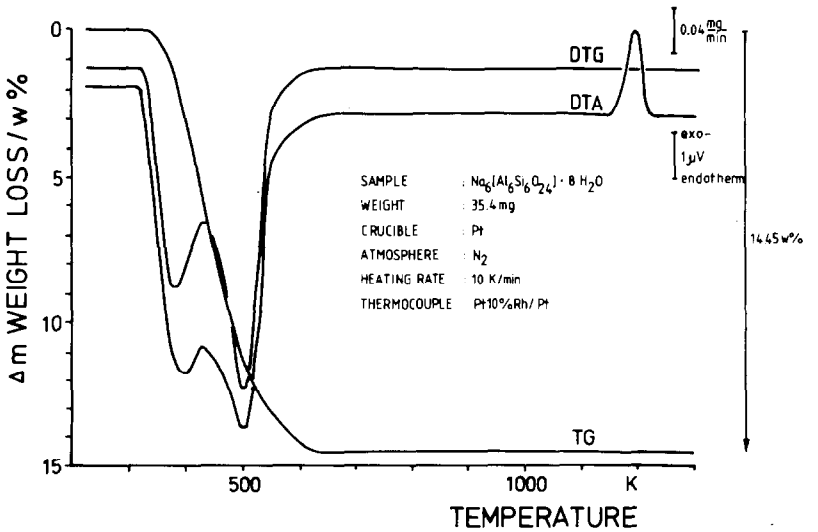

Fig. 3. Simultaneous thermoanalysis, TG(DTG)–DTA of the top-hydrate phase of the non-basic hydro-sodalite series, $Na_6[AlSiO_4]_6 \cdot 8H_2O$.

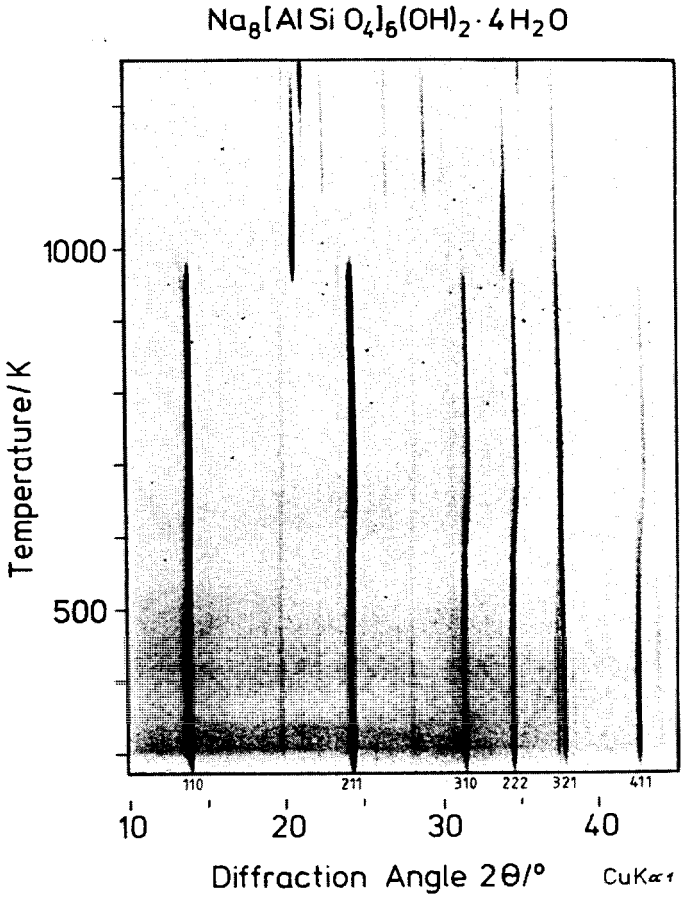

Fig. 4. X-ray diffraction heating photograph of the top-hydrate phase of the basic hydrosodalites, $Na_8[AlSiO_4]_6(OH)_2 \cdot 4H_2O$. Take notice of the diffuse intensities of reflections at temperatures around 650 K. Carnegieite at temperatures $T > 975$ K.

(Perkin Elmer 7025). Thin wafers of 0.1 mm thickness and 6 mm in diameter have been measured in the virgin state at 295 K under controlled atmosphere or vacuum conditions and at elevated temperatures of particular interest due to the thermoanalytical characteristics of individual phases.

Essential features of materials and experimental procedures of our investigations are shown in the flow-chart of Fig. 1.

RESULTS AND DISCUSSION

The thermoanalytical data of the two end-member series of the hydrosodalites at temperatures 300–1200 K are compared to each other in Figs. 2 and 3 (simultaneous thermoanalysis of TG/DTG, DTA) and Figs. 4 and 5

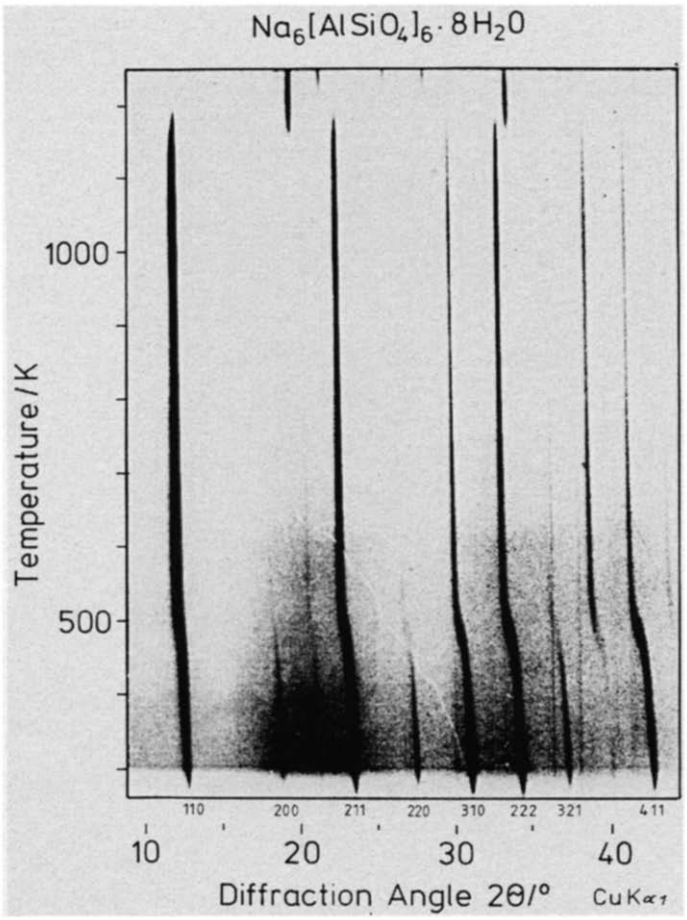

Fig. 5. X-ray diffraction heating photograph of the top-hydrate phase of the non-basic hydro-sodalites, $Na_6[AlSiO_4]_6 \cdot 8H_2O$. Carnegieite at temperatures $T > 1175$ K.

(high temperature X-ray diffraction photographs). Some preliminary results of the supplementary spectroscopic study (IR, NMR, neutron scattering) are shown in Figs. 6 and 7 (IR-transmission spectra in the region of 2000–4000 cm^{-1}). Comprehensive data on the individual phases of the hydro-sodalite family are given in Table 1.

The basic hydro-sodalites

Figure 2 shows the release of the hydrate water in the basic hydro-sodalites of starting composition $Na_8[AlSiO_4]_6(OH)_2 \cdot 4H_2O$ in a two-step decomposition reaction at temperatures of 420 and 650 K due to the DTG/DTA characteristics. The latter rather sluggish type of reaction yields the hydroxo-sodalite phase $Na_8[AlSiO_4]_6(OH)_2$, which decomposes in a first order reaction at 1020 K to the anhydrous material of composition

TABLE 1
The hydro-sodalite phases

Short notation	Chemical composition	Constitution formula	Crystal data	Conditions of syntheses	References
The basic hydro-sodalite series					
8:2:4	$Na_8[AlSiO_4]_6(OH)_2 \cdot 4H_2O$	$[HNa_4(OH)_3\square H]_2[AlSiO_4]_6$	cubic $P\bar{4}3n$, $Z=1$ $a_0 = 8.903(1)$Å, 295 K $a_0 = 8.884(1)$Å, 10 K	Mild hydrothermal condt. 1–200 atm., 350–600 K polycrystalline samples	Felsche and Luger (1986) [29] Felsche et al. (1986) [18]
8:2:2	$Na_8[AlSiO_4]_6(OH)_2 \cdot 2H_2O$	$[Na_4O_2H_3]_2[AlSiO_4]_6$	cubic $P\bar{4}3n$, $Z=1$ $a_0 = 8.890(1)$Å, 295 K	Hydrothermal conditions 1–5 kbar, 600—800 K single crystals	Hassan and Grundy (1983) [7]
Low temperature form			o-rhombic P222, $Z=1$ $a_0 = 8.925(6)b = 8.909(6)$ $a_0 = 8.870(6)$Å, 113 K		Bondareva and Malinovskii (1983) [8]
8:2:1.7	$Na_8[AlSiO_4]_6(OH)_2 \cdot 1.7H_2O$	$[ONa_4H][Na_4O_{2.7}H_{4.4}][AlSiO_4]_6$	cubic $P\bar{4}3n$, $Z=1$ $a_0 = 8.870(4)$Å, 293 K		Emiraliev and Yamzin (1978) [6]
8:2:0	$Na_8[AlSiO_4]_6(OH)_2$	$[ONa_4H]_2[AlSiO_4]_6$	cubic $P\bar{4}3n$, $Z=1$ $a_0 = 8.7342(8)$Å, 8 K	Dehydration of 8:2:4 or 8:2:2 samples at 775 K, vacuum, 1 week	Luger et al. (1986) [17]
The non-basic hydro-sodalite series					
6:0:8	$Na_6[AlSiO_4]_6 \cdot 8H_2O$	$[Na_3\square(OH_2)_4]_2[AlSiO_4]_6$	cubic $P\bar{4}3n$, $Z=1$ $a_0 = 8.8160(4)$Å, 10 K $a_0 = 8.854(1)$Å, 295 K $a_0 = 8.88(4)$Å, 293 K	Leaching of 8:2:4 samples in H_2O at 400 K in teflon coated auto-claves, repeatingly	Felsche et al. (1986) [24] Felsche and Luger (1986) [29]
6:0:0	$Na_6[AlSiO_4]_6$	$[Na_3\square][AlSiO_4]_6$	cubic P43n, $Z=1$ $a_0 = 9.122(1)$Å, 695 K	Thermal dehydration at 695 K, atmosphere, 12 h	Zhdanov et al. (1964) [3] Felsche and Luger (1986) [29] Baerlocher et al. (1986) [25]

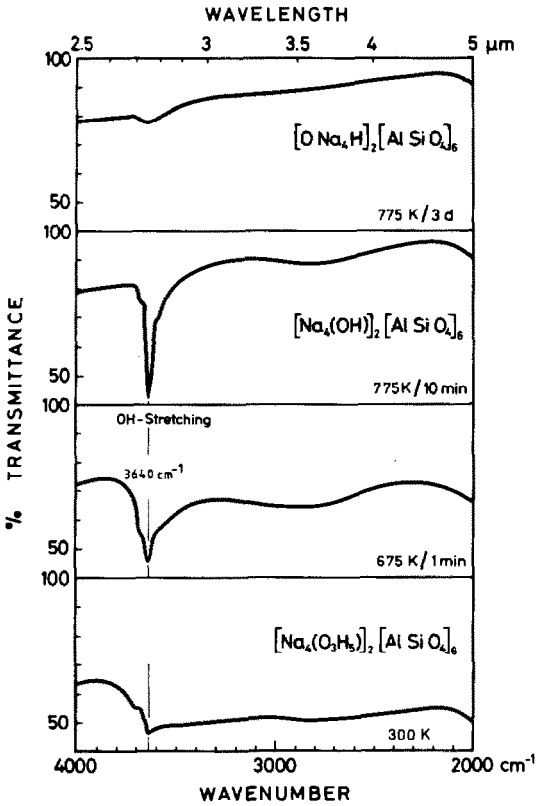

Fig. 6. IR-transmission spectra of the top-hydrate phase of the basic hydro-sodalites, $Na_8[AlSiO_4]_6(OH)_2 \cdot 4H_2O$ at room temperature and subsequent annealing of the sample at temperatures of special interest under vacuum conditions (*in situ* experiments).

$(Na_2O)_{1/6}Na[AlSiO_4]$ [12]. The X-ray pattern of this decomposition product (Fig. 4) shows close resemblance to the interstitial carnegieite phases, which have recently been identified up to a sodium oxide concentration of $(Na_2O)_{1/3}Na[AlSiO_4]_6$ [13].

Following the dehydration of the basic sodalite tetrahydrate $Na_8[AlSiO_4]_6(OH)_2 \cdot 4H_2O$ with the heating X-ray diffraction experiment, no significant change in the peak positions or intensities or reflexions shows up to temperatures of 550 K despite the 2.5% loss in weight of the sample due to the release of about 1.5 H_2O. Corresponding to the 650-K DTA peak, a drastic shrinkage in the cell volume is observed at temperatures of 500–750 K, however, with diffuse intensities shown by the main reflexions. The hydroxo-sodalite phase shows up at elevated temperatures, $700 < T < 975$ K, subsequently. Here again positions and intensities of the X-ray pattern remain unchanged despite the decreasing weight of the sample until decomposition to carnegieite occurs at temperatures of 975 K. Because of the different heating rates, the temperatures of the given phase transitions differ

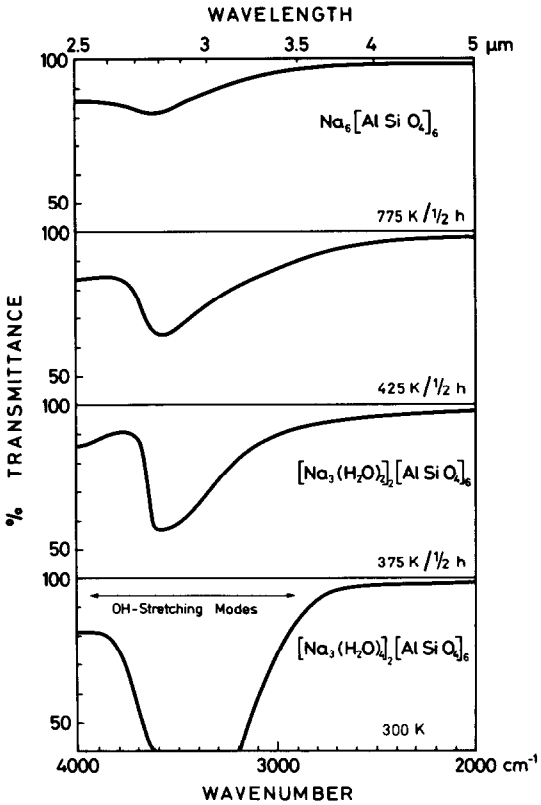

Fig. 7. IR-transmission spectra of the top hydrate phase of the non-basic hydro-sodalites, $Na_6[AlSiO_4]_6(OH)_2 \cdot 8H_2O$ at room temperature and subsequent annealing of the sample at temperatures of special interest under vacuum conditions (*in situ* experiments).

somewhat between the DTA/TG data and the heating X-ray photographs. It is also noteworthy that both the thermoanalytical methods work under open system (non-equilibrium) conditions. Accordingly, the single broad DTA-signal with a peak maximum at 650 K and as well as the sluggish slope of the TG-curve up to temperatures of 920 K indicate a rather complex nature of the dehydration mechanism and presumably high activation energies for the structural phase transition of the basic sodalite hydrates $Na_8[AlSiO_4]_6(OH)_2 \cdot nH_2O$ to the hydroxo-sodalite phase $Na_8[AlSiO_4]_6(OH)_2$.

The overall loss in weight of $4H_2O$ per formula unit $Na_8[AlSiO_4]_6(OH)_2 \cdot nH_2O$ during the dehydration corresponds to a decrease in cell volume of 5.2% in the basic sodalite hydrate series. It is this correspondence between the number and the size of the non-framework constituents and the unit cell volume which have the so-called basic sodalites [2] in common with the large number of natural occurring or synthetic sodalite-like phases. Several approaches and models of cooperative tilting and folding mechanisms have

been provided to gain a better understanding of this "positive interaction" of partial collapse of the sodalite structure which occurs upon extraction of the non-framework constituents (here $\Delta m = 4H_2O \sim \Delta V = -5.2\%$) or *vice versa* of extension of the framework which occurs upon isomorphous replacement by larger salt-like species or thermal expansion of the anhydrous sodalites [14,15,16]. Several structural analyses on the basic hydro-sodalite phases confirm the analogy with the family of the anhydrous sodalite compounds [6,7,8,17,18]. There is essentially no hydrogen bonding between the oxygens of OH^- and OH_2 groupings with those of the sodalite framework. Interesting positional variations of the oxygen and hydrogen atoms against each other and in respect to the tetrahedral organization of the four sodium ions per cage have been observed within the cubo-octahedral cavity of individual basic sodalite phases which differ in the contents of hydrate water. Figure 8 summarizes the structural findings of some of the basic and of the non-basic sodalites, respectively. The structural data on the configuration of the non-framework constituents at least of some of it may contribute to the understanding of the distinct thermoanalytical properties of the hydro-sodalite phases.

In contrast to the subhydrate phases, the tetrahydrate of the basic sodalite series freely releases some of the hydrate water in the first step of dehydration amounting to 2.5% loss in weight (Fig. 2)

$$Na_8[AlSiO_4]_6(OH)_2 \cdot 4H_2O \xrightarrow{420\ K} Na_8[AlSiO_4]_6(OH)_2 \cdot nH_2O,$$

$$2 < n < 4 + (4 - n)H_2O\uparrow$$

In the structure of $Na_8[AlSiO_4]_6(OD)_2 \cdot 4D_2O$ the sodium atoms are tightly bonded to the framework oxygens (Na–O = 234.0(6) pm) [18]. Accounting for all the non-framework constituents per sodalite cage, three hydroxyl groups (O–D) = 103(2) pm) and one hydrogen atom at the central position 2a of space group P$\bar{4}$3n (D–O = 115(2) pm, D–Na = 276.4(5) pm) (Fig. 8). The significance of the fifth hydrogen atom for the configuration of the complex cation $[HNa_4(OH)_3\square H]^{3+}$ or for the mechanism of the dehydration is not yet fully understood. (It is this hydrogen atom which could not be localized in the 10 K-neutron diffraction analysis of the tetrahydrate structure [18].) We argue, however, that the typical desorption character of the first dehydration step is correlated to the dynamical contact of this hydrogen atom to the 3OH groups and the corresponding ease in the release of up to $1H_2O$ from each sodalite cage

$$[HNa_4(OH)_3\square H]^{3+} \xrightarrow{420\ K} [HNa_4(OH)_2\square_2]^{3+} + H_2O\uparrow$$

The configuration of the non-framework constituents in the resulting product is obviously stable as long as there are more than two out of the four vertices of the non-sodium tetrahedron occupied by oxygen atoms within the statistical mean. Thus, the shrinkage of the framework is insignifi-

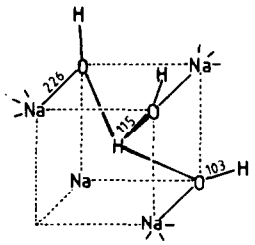

$Na_8[AlSiO_4]_6(OH)_2 \cdot 4\,H_2O$

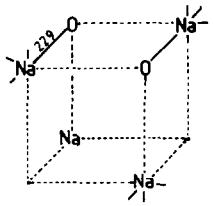

$Na_8[AlSiO_4]_6(OH)_2 \cdot 2\,H_2O$

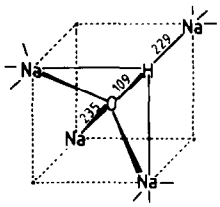

$Na_8[AlSiO_4]_6(OH)_2$

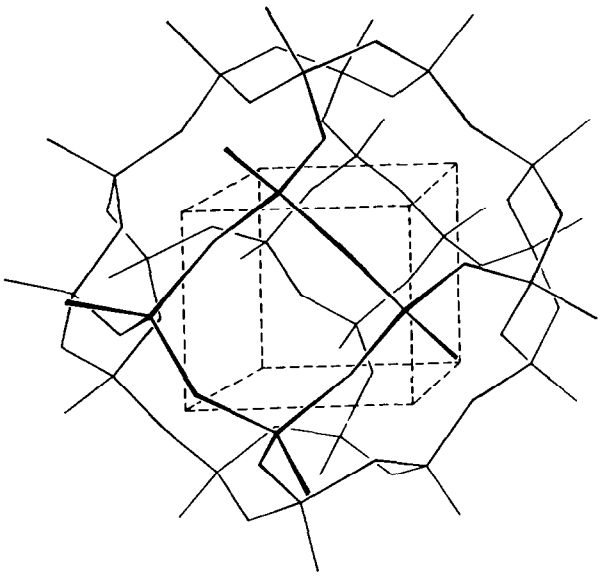

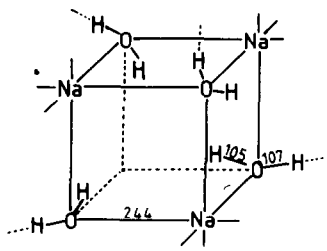

$Na_6[AlSiO_4]_6 \cdot 8\,H_2O$

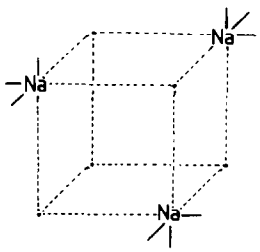

$Na_6[AlSiO_4]_6$

Fig. 8. Schematical drawing of the configuration of the non-framework constituents in the basic hydro-sodalite phases (upper section) of $Na_8[AlSiO_4]_6(OH)_2 \cdot 4H_2O$ [18], $Na_8[AlSiO_4]_6(OH)_2 \cdot 2H_2O$ [7] and $Na_8[AlSiO_4]_6(OH)_2$ [17]. The di-tetrahedral arrangements of the non-framework constituents are related to the sodalite framework [30,31] as shown in the middle section. Configurations of the non-framework constituents in the non-basic sodalite structures of $Na_6[AlSiO_4]_6 \cdot 8H_2O$ [24] and of $Na_6[AlSiO_4]_6$ [25] are shown in the lower section.

cant during the first period of dehydration at temperatures $T < 500$ K. However, a loss of additional hydrate water molecules corresponding to the weight loss of $\Delta m > 2.5\%$ with increasing temperatures at $T > 500$ K shown in the thermoanalytical run under open system conditions in Fig. 2

$$Na_8[AlSiO_4]_6(OH)_2 \cdot 2.2H_2O \xrightarrow{650\ K} Na_8[AlSiO_4]_6(OH)_2 \cdot nH_2O,$$
$$0 < n < 2 + (2.2 - n)H_2O\uparrow$$

yields a fundamental reorganization of the non-framework constituents with a significant shrinkage of the unit cell volume (Fig. 4). The structure of this dehydration product shows an empty centre position [7] which allows for the formulation for a complex cation $[\square Na_4O_2H_3]^{3+}$, or partial occupation of the centre position by hydrogen and oxygen atoms (neutron diffraction data on single crystals of arbitrary composition $Na_8[AlSiO_4]_6(OH)_2 \cdot 2H_2O$, [6]. This structural feature of substantially positional disorder of the non-framework constituents of oxygen and hydrogen atoms, which is verified with only single crystals being so far synthesized of hydro-sodalites, provides some intermediate character towards the final constitution in this series, which is given with the phase of the hydroxo-sodalite. The structure of $Na_8[AlSiO_4]_6(OH)_2$ shows the complex cation $[ONa_4H]^{3+}$ centred by the oxygen atom on position 2a on space group $P\bar{4}3n$ [17].

The diffuse character of the main reflexions in the heating photograph (Fig. 8) during the first period of the phase transition to the hydroxo-sodalite at temperatures of 420–600 K gives evidence for a protolytic type of decomposition reaction affecting the aluminosilicate framework. The mechanism might be governed by the hydrogen interactions with oxygen and sodium atoms which finally releases the excess water

$$[HNa_4(OH)_2\square_2]^{3+} \xrightarrow{450\ K} [\square Na_4O_2H_3\square_2]^{3+} \xrightarrow{600\ K} [ONa_4H\square_3]^{3+} + H_2O\uparrow$$

The corresponding ^{1}H-MAS-NMR experiments verify a substantial change in the chemical bound of the remaining hydrogen atom [19]. The chemical shift of -6.5 ppm in the hydroxo-sodalite phase as compared to the values of 3.5 and 1.0 ppm of the parent phase $Na_8[AlSiO_4]_6(OH)_2 \cdot 4H_2O$, respectively, allows for the assumption that the "common nature of bond" between the hydrogen and the oxygen atom of the previous hydrated hydroxyl groupings $[O_nH_{2n-1}]^-$ has diminished on account of a highly decoupled or isolated H atom. More information on the special stage of this hydrogen atom in the cubo-octahedral matrix of the sodalite cage will be given by the corresponding ^{1}H-NMR- and ESR-experiments.

The intermediate character of the dihydrate $Na_8[AlSiO_4]_6(OH)_2 \cdot 2H_2O$ within the series of basic sodalite hydrates is emphasized by the structural phase transition at 152 K (Fig. 9) which yields the change of the sodalite framework to orthorhombic symmetry. This partial collapse of the TO_4-framework might be advantageous because of the missing stabilization by

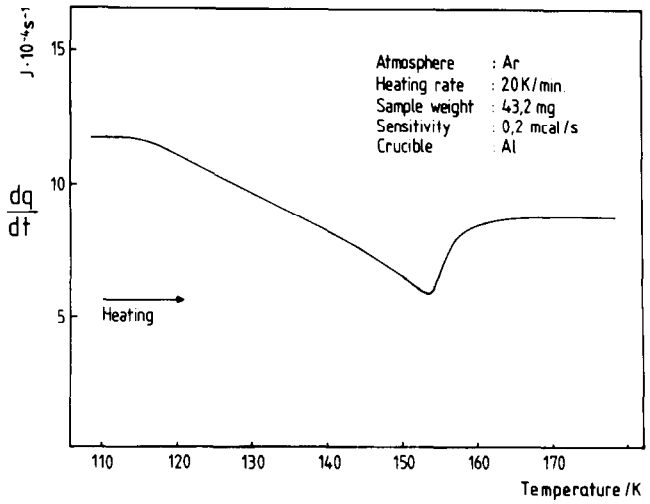

Fig. 9. Plot of the differential scanning calorimetry run of the "intermediate" type phase of the basic sodalite hydrates. $Na_8[AlSiO_4](OH)_2 \cdot 2H_2O$. Note that none of the hydro-sodalite phases of different composition shows any structural phase transition in the low temperature region of 5 K $< T <$ 300 K.

the remaining non-framework constituents. In the dihydrate phase of the basic sodalites the number of vertices of the ditetrahedron occupied by the four sodium atoms and the two oxygen atoms has dropped below or is equal to the value of 6. The four tetrahedral sodium atoms per sodalite cage obviously do not allow for the octahedral configuration of four sodium atoms and two additional oxygen atoms because of the tight binding to the oxygens of the six-membered rings of the sodalite framework. A micro-domain character of a low temperature form of the dihydrate sodalite has been discussed with the 120 K X-ray single crystal diffraction data [8]. Partial ordering of the H-atoms in the low- and in the high-temperature form of the basic sodalite dihydrate has been revealed by NMR-experiments [5,20].

The complex nature of the intra-cubooctahedral positioning and binding of the hydrogen atom with oxygen and sodium atoms is also elucidated by the IR-data given in Fig. 6. The *in situ* IR transmission spectra of the basic sodalite phases taken at arbitrary temperatures during the dehydration of the tetrahydrate $Na_8[AlSiO_4]_6(OH)_2 \cdot 4H_2O$ shows the increasing significance of the OH-stretching vibration at 3640 cm^{-1} with increasing temperature. The wavenumber and the O–H bond length correspond well with the data given for the hydro-garnets [21] and NaOH [22]. Notice that the 3640 cm^{-1} vibration is not shown in the non-basic hydro-sodalite spectra (Fig. 7). More extensive annealing of $t > 10$ min at the temperature of 775 K under vacuum conditions of 10^{-4} torr yields substantial decrease of this OH-stretching mode, subsequently. After annealing the basic sodalite sample for 3 days at 775 K the OH-stretching mode at 3640 cm^{-1} has diminished,

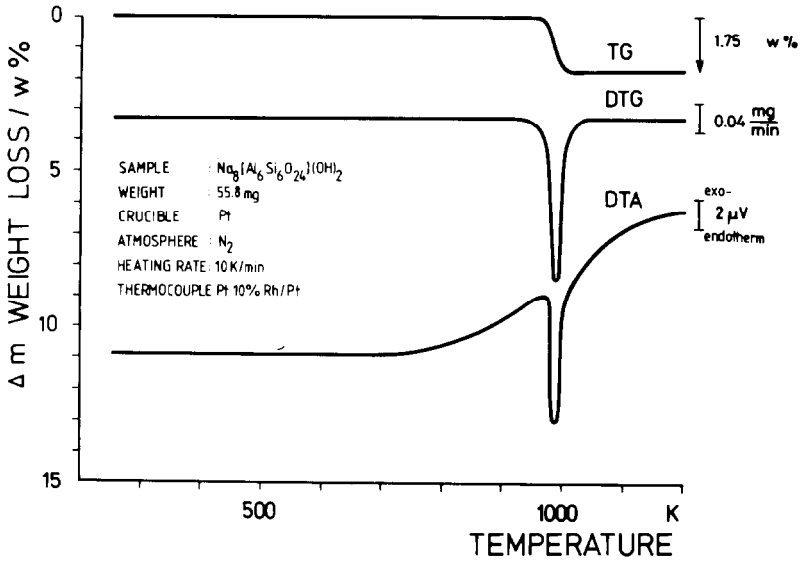

Fig. 10. Simultaneous thermoanalysis of the basic sodalite sample, which has been annealed for 3 days at 500 °C during the IR-high temperature study (Fig. 6).

substantially. The water contents corresponding to $1H_2O$ per formula unit is still available in the sample, however, as it is confirmed by the 1000 K decomposition step in Fig. 10. A verification of this peculiar finding might be given by the extended bond length of OH = 109 pm and the corresponding narrowing of the Na–H contacts of 228 pm in the hydroxo-sodalite structure [17].

The strongly time dependent reaction at 775 K in the IR study and as well the sluggish nature of the second decomposition stage (600–900 K) in the thermoanalytical experiment of Fig. 2 supports the model of partially hydrated hydroxyl groupings $[O_nH_{2n-1}]^-$ in the subsequent phases of composition $Na_8[AlSiO_4]_6(OH)_2 \cdot nH_2O$ with $0 < n < 2$. All the oxygens and hydrogens are located outside the Na_4-tetrahedron and show highly dynamic orientation against each other but no significant hydrogen bonding to the framework oxygens [5,7]. The dynamics of oxygen and hydrogen atoms at the interface between the Na_4-tetrahedron and the inner surface of the partially collapsed cubo-octahedron $[AlSiO_4]_3^{3-}$ obviously stabilizes the hydrated hydroxyl groupings. With increasing temperatures of 600 K $< T <$ 920 K (Fig. 2) or continuous annealing under isothermal conditions (775 K/75 h) the oxygens of the remaining OH^- groupings penetrate the faces of the Na_4-tetrahedron and occupy the centre position (2a of space group $P\bar{4}3n$), progressively, as shown for $Na_8[AlSiO_4]_6(OH_2)$ [17].

All the elastic scattering studies leave some questions open especially to the problem of the dynamics or the static statistical nature of the positions of Na, H and O atoms and their contacts within the sodalite cage. The

proceeding ^{1}H- and ^{23}Na-NMR and as well the quasi-elastic neutron scattering experiments will help to clarify this problem [19,23].

The non-basic hydro-sodalites

Contrary features show up for the non-basic hydro-sodalites $Na_6[SiAlO_4]_6 \cdot nH_2O$. Starting with the octa-hydrate all the eight molecules of hydrate water are released within a narrow temperature range of 350–550 K corresponding to the loss in weight of 14% from the TG-data (Fig. 3). DTG- and DTA-signals emphasize a two-step decomposition reaction with centres of gravity at temperatures of 375 and 500 K, respectively

$$Na_6[AlSiO_4]_6 \cdot 8H_2O \xrightarrow{375\ K} Na_6[AlSiO_4]_6 \cdot 4H_2O \xrightarrow{500\ K} Na_6[AlSiO_4]_6\ \text{sod.}$$

The X-ray diffraction heating photographs of Fig. 5 confirm drastic structural changes with the second step of the decomposition reaction at 500 K. Main reflections show a significant shift to lower diffraction angles, i.e. the unit cell volume increases(!) with the dehydration ($\Delta m = -8H_2O \sim \Delta V = +9.4\%$). Intensities of reflections 200, 220 and 321 diminish entirely, whereas novel reflections appear at this phase transition at temperatures $T > 500$ K (e.g. reflexion 400 at $2\theta = 39.4°$.

The essential features of the antagonistic effect of structure volume/concentration of hydrate water of the two end-member series of the hydro-sodalites have been assembled in Fig. 11.

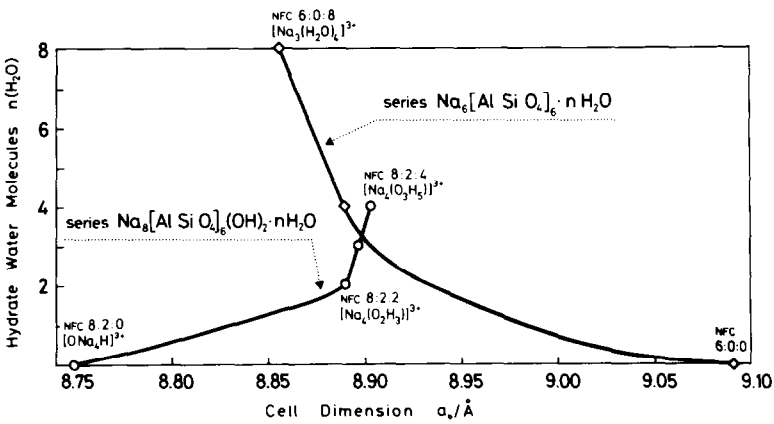

Fig. 11. Plot of the unit cell dimensions a_0 of the individual phases of both of the two end-member series of the hydro-sodalites against the molar concentration of hydrate water. Symbols of non-framework constituents (NFC) give the numbers of Na, OH and H_2O per formula unit $Na_{6+x}[AlSiO_4]_6(OH)_x \cdot nH_2O$ and the constitution of the so-called complex cation as found in the sodalite cavities of particular hydro-sodalite phases.

The significant expansion of the aluminosilicate framework in hydrosodalites $Na_6[SiAlO_4]_6 \cdot nH_2O$ upon dehydration is obviously correlated to the thermally induced destruction of the significant hydrogen bonding between the oxygen atoms of the hydrate water molecules (donators) and the framework oxygen atoms (acceptors). Recently, the 10 K-neutron diffraction study on the deuterized phase of the octa-hydrate yielded bond lengths of O_w–D = 107(4) pm and D...O_f = 194(4) pm, respectively [24]. The ditetrahedral arrangement of the non-framework constituents located in the truncated octahedral cavity of the sodalite structure is schematically represented in Fig. 8. The cation deficient complex of constitution $[Na_3\square(OH_2)_4]^{3+}$ retains the tetrahedral configuration of cations $[Na_3\square]^{3+}$ in the anhydrous sodalite in order to meet the topological and symmetry conditions of the truncated octahedral cage $[SiAlO_4]_3^{3+}$.

Related to the dehydration rate of $\Delta m = -8H_2O$ the alumosilicate framework shows a substantial relaxation of the Si–O–Al bridging angle from 136.2(3) to 156.3(6)°, as has recently been shown by a X-ray high-temperature diffraction study at 675 K employing advanced Rietveld profile-fitting techniques [26]. Ordering of the Si and Al atoms on the tetrahedral special positions 6d and 6c of space group $P\bar{4}3n$ has also been confirmed for the high temperature phase. This anhydrous high temperature form of the non-basic hydro-sodalite converts at 1175 K to carnegieite (Fig. 5). Notice the considerably lower temperature stability of the basic sodalite, which decomposes at 975 K. The exothermic phase transition

$$NaAlSiO_4(\text{sodalite}) \xrightarrow[\text{exo.(!)}]{1175\ K} NaAlSiO_4(\text{carnegieite})$$

reveals the metastable character of this novel sodalite compound, as compared to the known phases of composition $NaAlSiO_4$, nepheline and carnegieite, respectively [13].

Solid solutions

The constitution formula generally accepted for the phases of the hydrosodalite family $Na_{6+x}[AlSiO_4]_6(OH)_x \cdot nH_2O$ [2] implies the solid solution character for coefficients x and n and correlated steady variation in the properties of corresponding samples. We have shown above that the two end-members of the solid solution series (end-members in respect to the concentration of xNaOH) exhibit an opposite but continuous variation of unit cell volume with variation of the water content n upon thermal dehydration. Partially leached samples showing NaOH concentrations with varying x values $0 < x < 2$ and arbitrary water contents $3 < n < 5$ reveal homogeneous character at low temperatures $100 < T < 400$ K from DSC- and X-ray powder diffraction examinations. At elevated temperatures de-

composition occurs, however, with corresponding samples. Figure 12 shows the decomposition of a sample of composition $Na_7[AlSiO_4]_6(OH) \cdot 4H_2O$

$$2\ Na_7[AlSiO_4]_6(OH) \cdot 4H_2O \xrightarrow[\text{open system}]{475\ K} Na_8[AlSiO_4]_6(OH)_2 \cdot 2H_2O + Na_6[AlSiO_4]_6 + 6H_2O\uparrow$$

The bifurcation in the slope of the curves showing the dependence of the unit cell volumes versus water contents in the two end-member series of the hydro-sodalite system (Fig. 11) is immediately reflected by the separation of the main reflections 110 and 211 at the arbitrary temperature of 475 K in Fig. 12.

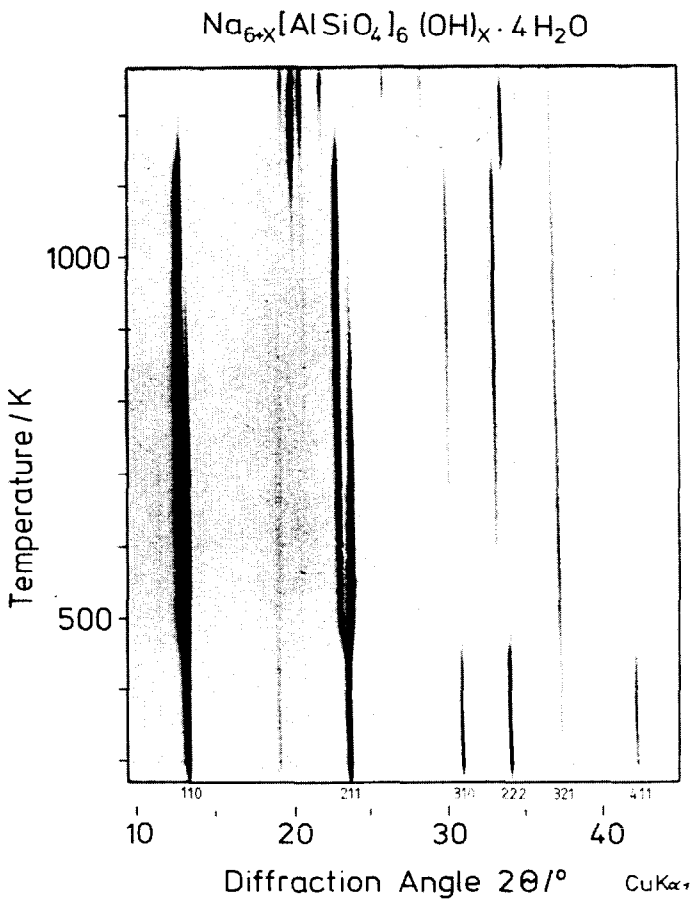

Fig. 12. X-ray diffraction heating photograph of the hydro-sodalite solid solution phase of composition $Na_7[AlSiO_4]_6(OH) \cdot 4H_2O$. Notice the phase separation at 475 K and subsequent decomposition of the basic sodalite contribution at temperatures of 975 K and of the non-basic sodalite contribution of the sample at considerably higher temperatures of 1150 K. Carnegieite at temperatures $T > 1175$ K.

Concerning the thermodynamics of the hydro-sodalite system it seems worthwhile mentioning that phases of the basic hydro-sodalite series are the intrinsic phases from the syntheses. Basic sodalites of composition $Na_8[AlSiO_4]_6(OH)_2 \cdot 4H_2O$ or $Na_8[AlSiO_4]_6(OH) \cdot nH_2O$ with arbitrary values of $1.7 < n < 2.2$ from thermogravimetric analyses, but stoichiometric value of $n = 2H_2O$, hypothetically, are the only crystalline phases ever observed from hydrothermal syntheses so far. The latter composition occurs at elevated temperatures and pressures of $625 < T < 875$ K and $0.1 < p < 5$ kbar (single crystals of several millimeters in size in 100–1000 cm^3 autoclave volumes!). The tetrahydrate basic sodalite samples employed in the dehydration or exchange experiments occur in polycrystalline quality (0.01–10 μ) under mild hydrothermal conditions, exclusively. Whether the two given compounds exhibit temperature/pressure polymorphs of the given system has not been clarified yet because of the large alkali-water excess concentration needed in the successful syntheses. All the remaining compounds discussed in the context with the hydro-sodalite family occur from thermal decomposition (hydroxo-sodalite of composition 8 : 2 : 0!) or exchange experiments (non-basic hydro-sodalites of composition 6 : 0 : n!). The thorough leaching of $NaOH \cdot nH_2O$ in reiterating exchange experiments and analyses of the pH-value of the leaching water is one of the conditions necessary for the yield of pure-phase non-basic sodalites $Na_6[AlSiO_4]_6 \cdot nH_2O$, a condition which obviously had not been met in previous studies on so-called hydro-sodalites [3,25], because of the misleading assumption of solid solution character for arbitrary values $0 < x < 2$ of the hydro-sodalite family. It is just the procedure of thermal activations of materials at elevated temperatures of 500–850 K which reveal some evidence of mixed phase samples used in the studies of corresponding sorption properties instead of the so-called "Zh-sodalite" composition $Na_6[AlSiO_4]_6 \cdot nH_2O$.

Resorption experiments compensating for the given dehydration study here have not yet been completed because of the long time character of the sorption experiments in reaching equilibrium of all the dehydrated samples with gaseous H_2O. Preliminary results of the proceeding sorption study show some evidence for a different constitution of resorbed water in samples of the basic hydro-sodalite series as compared with the constitution of complex aqueous hydroxyl groupings $[O_nH_{2n-1}]^-$ of the starting products.

In order to demonstrate the relevance of the given sodalite data with the thermal behaviour of more complicated zeolites, we show thermal dehydration characteristics of zeolite A in Fig. 13. The sample had been saturated with H_2O at 300 K and subsequently heated to 1100 K on the thermobalance as well as on the Guinier X-ray diffraction heating camera under dry nitrogen atmosphere. In the low temperature range of 300–450 K the unit cell volume shows drastic decrease with the release of a percentage of adsorbed water molecules but a distinct increase at temperatures 374–440 K in the course of further release of water. Regular thermal expansion char-

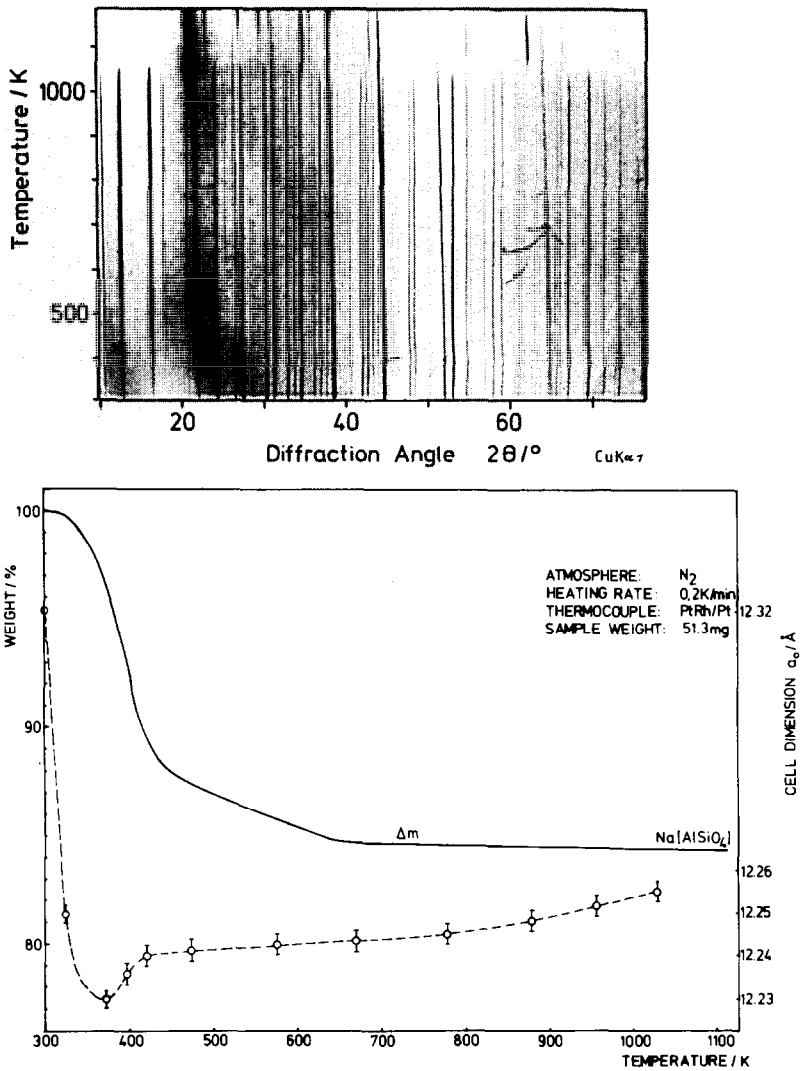

Fig. 13. Thermoanalytical data of the structurally related zeolite A. X-ray diffraction heating photograph (upper section) shows the discontinuity of the pattern at 375 K and the decomposition to a carnegieite-like phase at temperatures of 1050 K. The corresponding loss in weight from dehydration by thermogravimetry and the quantitative evaluation of the heating X-ray diffraction photograph of a_0 of a sample of the same batch is shown below.

acteristics of values 2.5 10^{-6} K^{-1} are observed at temperatures 450–1050 K. This effect shows some resemblance with the antagonistic behaviour of the hydro-sodalites shown in Fig. 11. Presumably the hydrogen bonding within the β-cage is destroyed at temperatures 375–440 K, thus giving rise to the significant relaxation of the zeolite A framework structure. This finding is

not well understood in terms of the recently given X-ray high temperature data [27,28] nor of the NMR-results on those materials [26]. Similar findings of contraction and subsequent expansion of the framework have recently been also shown in the dehydration characteristics of the structurally related zeolite X [28]. Some further studies are necessary in order to reveal the complex mechanisms of interchanges of coupled β-/α-cage effects in this type of porous tectosilicate. Combined ^{1}H-/^{23}Na-NMR and quasi-elastic neutron scattering experiments on samples of particular sorption properties are underway.

ACKNOWLEDGEMENTS

We thank G.O. Brunner, ETH-Zürich, for the support of the IR-data and the thorough discussion of experimental details. The thermo-analytical experiments have been carried out by G. Wildermuth, and essential support in the X-ray diffraction procedure has been provided by A. Straub. Helpful assistance of W. Zieger in the preparation of samples and of H. Fendrich in the graphical representation of results in Fig. 8 is also gratefully acknowledged.

REFERENCES

1 W. Borchert and J. Keidel, Heidelberg. Beitr. Mineral Petrogr., 1 (1947) 2.
2 R.M. Barrer and E.A.D. White, J. Chem. Soc., 286 (1952) 1561.
3 S.P. Zhdanov, N.N. Buntar and E.N. Egorova, Zh. Dokl. Akad. Naukn. SSSR., 154 (1964) 419.
4 R.M. Barrer, J.F. Cole and H. Sticher, J. Chem. Soc. A, (1968) 2475.
5 V.Yu. Galitskii, B.N. Grechushnikov, V.V. Ilyukhin and N.V. Belov, Sov. Phys. Dokl., 19 (1974) 111.
6 A. Emiraliev and I.I. Yamzin, Sov. Phys. Crystallogr., 23 (1978) 27.
7 I. Hassan and H.D. Grundy, Acta Crystallogr., Sect. C, 39 (1983) 3.
8 O.S. Bondareva and Yu.A. Malinovskii, Sov. Phys. Crystallogr., 28 (1983) 273.
9 S. Luger and J. Felsche, Acta Crystallogr., Sect. A, 40 (1984) C116.
10 H. Eppler and H. Selhofer, Thermochim. Acta, 20 (1977) 45.
11 G.O. Brunner, H. Reifler and E. Klebler, Rev. Sci. Instrum., 57 (1986) 295.
12 D.J. Schipper, T.W. Lathouwers and C.Z. van Doorn, J. Am. Ceram. Soc., 56 (1973) 523.
13 R. Klingenberg and J. Felsche, J. Solid State Chem., 61 (1986) 40.
14 C.M.B. Henderson and D. Taylor, Spectrochim. Acta, Part A, 33 (1977) 283.
15 C.M.B. Henderson and D. Taylor, Phys. Chem. Min., 2 (1978) 337.
16 W. Depmeier, Acta Crystallogr., Sect. B40 (1984) 185; W. Depmeier, Acta Crystallogr., Sect. B41 (1985) 101.
17 S. Luger, J. Felsche and P. Fischer, Acta Crystallogr., Sect. C, 43 (1987) 1.
18 J. Felsche, P. Fischer and S. Luger, Acta Crystallogr., submitted.
19 Ch. Buhl, J. Felsche, S. Luger and H. Foerster, Zeolites, submitted.

20 V.Yu. Galitskii, V.N. Shcherbakov and S.P. Gabuda, Sov. Phys. Crystallogr., 17 (1973) 691.
21 P.C. Cohen-Addad and P. Ducros, Acta Crystallogr., 23 (1967) 220.
22 R.A. Buchanan, J. Chem. Phys., 31 (1959) 870.
23 W. Buehrer, S. Luger and J. Felsche, J. Chem. Phys., (1987) in press.
24 J. Felsche, P. Fischer and S. Luger, Acta Crystallogr., Sect. C, 43 (1987) in press.
25 Ch. Baerlocher, J. Felsche and S. Luger, Zeolites, 6 (1986) 367.
26 W. Oehme, D. Michel, H. Pfeifer and S.P. Zhdanov, Zeolites, 4 (1984) 120.
27 J.M. Adams and D.A. Haselden, J. Solid State Chem., 51 (1984) 83.
28 J.J. Pluth and J.V. Smith, J. Am. Chem. Soc., 105 (1983) 1192.
29 J. Felsche and S. Luger, Ber. Dtsch. Bunsenges. Phys. Chem., 90 (1986) 731.
30 L. Pauling, Z. Kristallogr., 74 (1930) 213.
31 J. Löns and H. Schulz, Acta Crystallogr., 23 (1967) 434.